Generation of broadband spontaneous parametric fluorescence using multiple bulk nonlinear crystals

Masayuki Okano,[1,2] **Ryo Okamoto,**[1,2] **Akira Tanaka,**[1,2]
Shanthi Subashchandran,[1,2] **and Shigeki Takeuchi**[1,2,*]

[1]*Research Institute for Electronic Science, Hokkaido University, Sapporo 001-0020, Japan*
[2]*The Institute of Scientific and Industrial Research, Osaka University, Osaka 567-0047, Japan*
[*]*takeuchi@es.hokudai.ac.jp*

Abstract: We propose a novel method for generating broadband spontaneous parametric fluorescence by using a set of bulk nonlinear crystals (NLCs). We also demonstrate this scheme experimentally. Our method employs a superposition of spontaneous parametric fluorescence spectra generated using multiple bulk NLCs. A typical bandwidth of 160 nm (73 THz) with a degenerate wavelength of 808 nm was achieved using two β-barium-borate (BBO) crystals, whereas a typical bandwidth of 75 nm (34 THz) was realized using a single BBO crystal. We also observed coincidence counts of generated photon pairs in a non-collinear configuration. The bandwidth could be further broadened by increasing the number of NLCs. Our demonstration suggests that a set of four BBO crystals could realize a bandwidth of approximately 215 nm (100 THz). We also discuss the stability of Hong-Ou-Mandel two-photon interference between the parametric fluorescence generated by this scheme. Our simple scheme is easy to implement with conventional NLCs and does not require special devices.

OCIS codes: (190.4410) Nonlinear optics, parametric processes; (270.0270) Quantum optics.

References and links

1. E. Knill, R. Laflamme, and G. Milburn, "A scheme for efficient quantum computation with linear optics," Nature **409**(6816), 46–52 (2001).
2. L.-M. Duan, M. Lukin, J. Cirac, and P. Zoller, "Long-distance quantum communication with atomic ensembles and linear optics," Nature **414**(6862), 413–418 (2001).
3. S. E. Harris, "Chirp and compress: Toward single-cycle biphotons," Phys. Rev. Lett. **98**(6), 063602 (2007).
4. G. Brida, V. Caricato, M. V. Fedorov, M. Genovese, M. Gramegna, and S. P. Kulik, "Characterization of spectral entanglement of spontaneous parametric-down conversion biphotons in femtosecond pulsed regime," Europhys. Lett. **87**(6), 64003 (2009).
5. M. B. Nasr, B. E. A. Saleh, A. V. Sergienko, and M. C. Teich, "Demonstration of dispersion-canceled quantum-optical coherence tomography," Phys. Rev. Lett. **91**(8), 083601 (2003).
6. B. Dayan, A. Pe'er, A. A. Friesem, and Y. Silberberg, "Two photon absorption and coherent control with broadband down-converted light," Phys. Rev. Lett. **93**(2), 023005 (2004).
7. S. M. Hendrickson, M. M. Lai, T. B. Pittman, and J. D. Franson, "Observation of two-photon absorption at low power levels using tapered optical fibers in rubidium vapor," Phys. Rev. Lett. **105**(17), 173602 (2010).
8. V. Giovannetti, S. Lloyd, L. Maccone, and F. N. C. Wong, "Clock synchronization with dispersion cancellation," Phys. Rev. Lett. **87**(11), 117902 (2001).

#167526 - $15.00 USD Received 26 Apr 2012; revised 18 May 2012; accepted 21 May 2012; published 8 Jun 2012

9. N. Mohan, O. Minaeva, G. Goltsman, M. Saleh, M. Nasr, A. Sergienko, B. Saleh, and M. Teich, "Ultrabroadband coherence-domain imaging using parametric downconversion and superconducting single-photon detectors at 1064 nm," Appl. Opt. **48**(20), 4009–4017 (2009).
10. M. Nasr, S. Carrasco, B. Saleh, A. Sergienko, M. Teich, J. Torres, L. Torner, D. Hum, and M. Fejer, "Ultrabroadband biphotons generated via chirped quasi-phase-matched optical parametric down-conversion," Phys. Rev. Lett. **100**(18), 183601 (2008).
11. A. M. Brańczyk, A. Fedrizzi, T. M. Stace, T. C. Ralph, and A. G. White, "Engineered optical nonlinearity for quantum light sources," Opt. Express **19**(1), 55–65 (2011).
12. K. G. Katamadze and S. P. Kulik, "Control of the spectrum of the biphoton field," JETP **112**(1), 20–37 (2011).
13. E. Dauler, G. Jaeger, A. Muller, A. Migdall, and A. Sergienko, "Tests of a two-photon technique for measuring polarization mode dispersion with subfemtosecond precision," J. Res. Natl. Inst. Stand. Technol. **104**(1), 1–10 (1999).
14. S. Carrasco, M. B. Nasr, A. V. Sergienko, B. E. A. Saleh, M. C. Teich, J. P. Torres, and L. Torner, "Broadband light generation by non-collinear parametric downconversion," Opt. Lett. **31**(2), 253–255 (2006).
15. M. Hendrych, X. Shi, A. Valencia, and J. Torres, "Broadening the bandwidth of entangled photons: A step towards the generation of extremely short biphotons," Phys. Rev. A **79**(2), 023817 (2009).
16. K. O'Donnell and A. U'Ren, "Observation of ultrabroadband, beamlike parametric downconversion," Opt. Lett. **32**(7), 817–819 (2007).
17. C. Hong, Z. Ou, and L. Mandel, "Measurement of subpicosecond time intervals between two photons by interference," Phys. Rev. Lett. **59**(18), 2044–2046 (1987).
18. R. Boyd, *Nonlinear Optics* (Academic Press, 2003).
19. S. Baek and Y. Kim, "Spectral properties of entangled photon pairs generated via frequency-degenerate type-i spontaneous parametric down-conversion," Phys. Rev. A **77**(4), 043807 (2008).
20. G. D. Giuseppe, M. Atatüre, M. D. Shaw, A. V. Sergienko, B. E. A. Saleh, and M. C. Teich, "Entangled-photon generation from parametric down-conversion in media with inhomogeneous nonlinearity," Phys. Rev. A **66**(1), 013801 (2002).
21. Y.-H. Kim, S. P. Kulik, and Y. Shih, "High-intensity pulsed source of space-time and polarization double-entangled photon pairs," Phys. Rev. A **62**(1), 011802 (2000).
22. R. Rangarajan, M. Goggin, and P. Kwiat, "Optimizing type-I polarization-entangled photons," Opt. Express **17**(21), 18920–18933 (2009).
23. P. G. Kwiat, E. Waks, A. G. White, I. Appelbaum, and P. H. Eberhard, "Ultrabright source of polarization-entangled photons," Phys. Rev. A **60**(2), R773–R776 (1999).
24. Y. Kawabe, H. Fujiwara, R. Okamoto, K. Sasaki, and S. Takeuchi, "Quantum interference fringes beating the diffraction limit," Opt. Express **15**(21), 14244–14250 (2007).
25. H. Fujiwara, Y. Kawabe, R. Okamoto, S. Takeuchi, and K. Sasaki, "Quantum lithography under imperfect conditions effects of loss and dephasing on two-photon interference fringes," J. Opt. Soc. Am. B **28**(3), 422–431 (2011).
26. M. Atatüre, A. V. Sergienko, B. E. A. Saleh, and M. C. Teich, "Entanglement in cascaded-crystal parametric down-conversion," Phys. Rev. Lett. **86**(18), 4013–4016 (2002).
27. A. Steinberg, P. Kwiat, and R. Chiao, "Dispersion cancellation and high-resolution time measurements in a fourth-order optical interferometer," Phys. Rev. A **45**(9), 6659–6665 (1992).
28. A. Pe'er, Y. Bromberg, B. Dayan, Y. Silberberg, and A. A. Friesem, "Broadband sum-frequency generation as an efficient two-photon detector for optical tomography," Opt. Express **15**(14), 8760–8769 (2007).
29. R. Kaltenbaek, J. Lavoie, D. N. Biggerstaff, and K. J. Resch, "Quantum-inspired interferometry with chirped laser pulses," Nat. Phys. **4**(11), 864–868 (2008).

1. Introduction

Quantum entangled photon pairs play a key role in quantum information processing [1] and quantum communication [2]. In recent years, entangled photon pairs with ultrabroad bandwidths in the frequency domain have attracted much attention [3, 4]. Such frequency-entangled photon pairs are indispensable for the future realization of "single-cycle biphotons" [3], whose characteristic coincidence time, as measured at distant detectors, is a single optical cycle. These broadband correlated photon pairs have the potential to realize high-resolution quantum optical coherence tomography [5], highly-efficient two-photon absorption experiments [6, 7], and precise synchronization of two clocks [8].

Various methods have been developed for generating broadband spontaneous parametric fluorescence that can be used as correlated photon pairs. However, there have been only a few methods that can realize an ultrabroad bandwidth of an order of 100 THz. For example, one

#167526 - $15.00 USD Received 26 Apr 2012; revised 18 May 2012; accepted 21 May 2012; published 8 Jun 2012

method uses chirped quasi-phase matched devices. It was theoretically proposed by S.E. Harris [3] and subsequently demonstrated experimentally by generating ultrabroadband spontaneous parametric fluorescence in the range 700-1500 nm with a center wavelength λ_c of 1064 nm [9] and 300 nm (136 THz) bandwidth spontaneous parametric fluorescence at λ_c = 812 nm [10]. Although this approach is suitable for ultrabroadband generation and enables us to engineer the high optical nonlinearities of materials [11], it requires sophisticated quasi-phase matched devices that should be properly designed for a specific purpose. Furthermore, it is difficult to use this method to the applications where the pump laser wavelength has to be varied over a certain range ($>$10 nm). Another method employs a large temperature modulation in a NLC and obtained a broad bandwidth of 253 nm (154 THz) at λ_c = 702 nm [12]. However, this method also requires sophisticated device structure to exploit spatial modulation of temperature in a tiny NLC. Although a broad bandwidth of 174 nm (106 THz) at λ_c = 702 nm was reported using an ultrathin (thickness: 0.05 mm) crystal [13], this method increases the bandwidth at the expense of the photon flux.

There have been other experimental demonstrations towards the generation of broadband spontaneous parametric fluorescence. One approach is to control the pump beam incident angles to obtain a wide range of the phase matching conditions. A method using tightly focused pump beam was reported with 84 THz bandwidth [14], and another method uses a pair of gratings for pump (24 THz [15]). Oppositely, one can collect the parametric fluorescence spread over in a certain divergence angle (91 THz [16]).

In this paper, we propose a novel method that uses multiple bulk NLCs to generate broadband spontaneous parametric fluorescence. Our scheme is easy to implement as it employs a set of conventional bulk NLCs and it does not require special devices. This scheme uses a weakly focused pump beam and the broadband photons are emitted into a certain direction in a non-collinear configuration, so that the parametric fluorescence can be coupled into single mode fiber couplers. In principle, the bandwidth can be extended by increasing the number of NLCs up to 100 THz as is shown later. Furthermore, the pump laser frequency can be tuned within the tuning range of the phase-matching conditions of NLCs. We then experimentally demonstrate the scheme by using two bulk NLCs. A typical bandwidth of 160 nm (73 THz) with a degenerate wavelength of 808 nm was achieved using two β-barium-borate (BBO) crystals. We also measured the coincidence counts of generated photon pairs in a non-collinear configuration. Calculations based on the experimental results suggest that it should be possible to realize a bandwidth of approximately 215 nm (100 THz) by using a set of four BBO crystals.

We also discuss the effect of air gaps between multiple NLCs on the Hong-Ou-Mandel (HOM) interference [17] between the daughter photons generated by our scheme. Our theoretical analysis suggests that the difference in the refractive indices of the air for the pump light and the daughter photons indeed modify the shape of the HOM interference, but the change is negligibly small for the current experimental condition. The analysis also suggests that the effect of group velocity mismatch between the pump light and the daughter photon is also negligible and it is not necessary to stabilize the distance between crystals with interferometric accuracy when a pump light with appropriate coherence length is used.

The remainder of the paper is organized as follows. Section 2 describes the proposed scheme. Section 3 describes the experimental setup used to demonstrate the scheme by using two bulk NLCs. Section 4 presents the experimental results and discussions about the effect of the air gap between NLCs. The final section summarizes the findings of this study and gives the conclusions.

#167526 - $15.00 USD Received 26 Apr 2012; revised 18 May 2012; accepted 21 May 2012; published 8 Jun 2012

2. Proposed scheme

For bulk NLCs, the spontaneous parametric fluorescence spectrum is determined by the phase-matching conditions for parametric down conversion, which is a second-order nonlinear process. A pump photon with a frequency ω_p and a momentum k_p is down converted to a pair of photons, which are signal and idler photons with frequencies ω_s and ω_i and momenta k_s and k_i, respectively. Due to energy conservation, $\omega_p = \omega_s + \omega_i$ must be satisfied so that the momentum mismatch $\Delta k = k_p - k_s - k_i$ must be zero to satisfy the critical phase-matching condition [18]. The frequency spectrum $F(\omega)$ for spontaneous parametric fluorescence, which consists of pairs of signal $F(\omega_s)$ and idler $F(\omega_i)$ photons, can be assumed to be symmetric relative to the center frequency $\frac{\omega_p}{2}$. The spectrum $F(\omega)$, which is $F(\omega_s) = F(\omega_i) = F(\frac{\omega_p}{2} \pm \Omega) = F(\Omega)$, can then be described as

$$F(\Omega) \propto \left| \int_0^L dz \exp\left[i\Delta k(\Omega) z \right] \right|^2 = L^2 \mathrm{sinc}^2 \left[\frac{\Delta k(\Omega) L}{2} \right], \tag{1}$$

where z is the position in the NLC along the pump beam axis. and L is the length of the NLC along the z axis. The momentum mismatch Δk in the NLC depends on the frequencies of the generated signal and idler photons. Thus, the frequency spectrum $F(\omega)$ has a finite bandwidth that is determined by the frequency-dependent momentum mismatch $\Delta k(\Omega)$.

We now propose our scheme that employs multiple NLCs to generate broadband spontaneous parametric fluorescence. As an example, Fig. 1 schematically depicts the proposed method for three NLCs. Multiple bulk NLCs are aligned in parallel along the pump beam. The phase-matching condition, which depends on the momentum mismatch Δk, for each NLC can be controlled by controlling the tilt angle θ_t of the optic axis of the NLC. The tilt angle between the optic axis and the pump beam is varied in the horizontal plane (i.e., parallel to the page) and the pump beam is horizontally polarized in Fig. 1. The tilt angles of the three NLCs are set to be different from each other (θ_{ta}, θ_{tb}, and θ_{tc} in Fig. 1). Consequently, the parametric fluorescence spectra generated by the NLCs will differ due to the phase-matching conditions. The parametric fluorescence generated from all the NLCs can be collected at an emission angle $\theta(-\theta)$ as signal (idler) photons of correlated photon pairs in a non-collinear configuration. The parametric fluorescence spectrum also depends on the emission angle θ, which determines the momentum direction of generated photons. Thus, the signal photon spectra generated from the NLCs and detected at an emission angle $\theta = \theta_d$, can be expressed by

$$F(\Omega, \theta_d) = \sum_{i=a,b,c} F_i(\Omega, \theta_d, \theta_{ti}) \propto \sum_{i=a,b,c} L^2 \mathrm{sinc}^2 \left[\frac{\Delta k_i(\Omega, \theta_d, \theta_{ti}) L}{2} \right], \tag{2}$$

where F_i, θ_{ti}, and k_i are the signal photon spectrum, the NLC tilt angle, and the momentum mismatch of the ith NLC ($i = a, b, c$), respectively. By suitably controlling the phase-matching conditions of the NLCs, the spontaneous parametric fluorescence bandwidth could be broadened due to the superposition of spontaneous parametric fluorescence generated from the multiple bulk NLCs.

Figure 2 schematically depicts the proposed scheme with three NLCs in the view of the frequency spectrum. The upper left figure of Fig. 2 shows the relation between the emission angle θ and the wavelength λ of the generated parametric fluorescence as tuning curves that indicate the phase-matching conditions. The three different tilt angles θ_t of the three NLCs ($\theta_{ta}, \theta_{tb}, \theta_{tc}$) lead to three different tuning curves. When the generated signal and idler photons are collected at emission angles of $\theta = \theta_d$ and $-\theta_d$, respectively, the parametric fluorescence spectra generated by the NLCs have different peaks and bandwidths, as shown in the lower left figure of Fig. 2. The broadband spontaneous parametric fluorescence can be obtained at

#167526 - $15.00 USD Received 26 Apr 2012; revised 18 May 2012; accepted 21 May 2012; published 8 Jun 2012

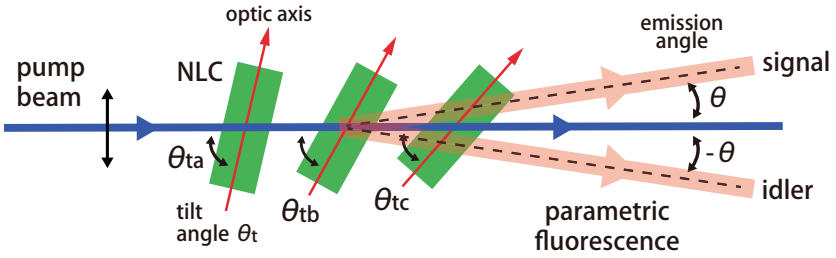

Fig. 1. Schematic of proposed method to generate spontaneous parametric fluorescence by using multiple bulk NLCs. Multiple (three in figure) bulk NLCs are aligned in parallel; the pump beam passes through all the NLCs. The optic axes of the NLCs have different tilt angles θ_t ($\theta_{ta}, \theta_{tb}, \theta_{tc}$) to control the phase-matching condition for each NLC. Generated parametric fluorescence is collected at the emission angle $\pm\theta$ as signal and idler photons.

the detection angle θ_d as a superposition of these spectra, as shown in the lower right figure of Fig. 2. Following the proposed method, the spectral bandwidth can be broadened by increasing the number of crystals. The expected broadening of the bandwidth with increasing number of crystals will be discussed later in Sec. 4.1 based on experimentally measured spectra.

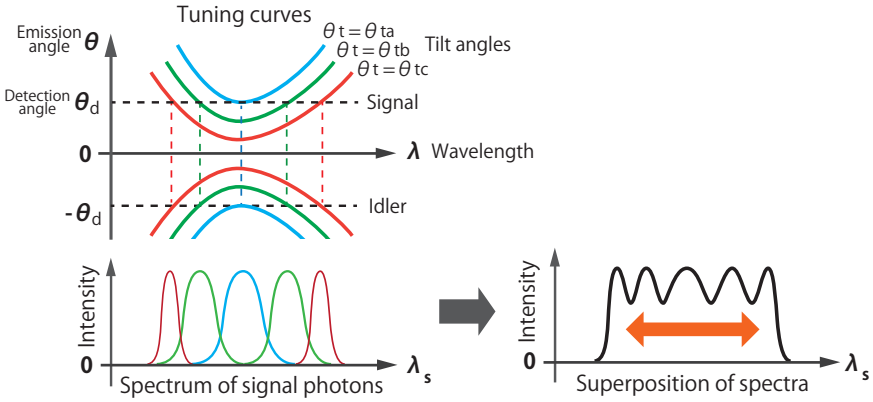

Fig. 2. Illustration of proposed scheme for generating spontaneous parametric fluorescence using three bulk NLCs. Upper left figure shows tuning curves of three NLCs with tilt angles θ_t of θ_{ta}, θ_{tb}, and θ_{tc}. Lower left figure shows corresponding parametric fluorescence spectra from these three NLCs for a detection angle $\theta = \pm\theta_d$. Lower right figure shows broadened spectrum as a superposition of these spectra.

3. Experimental setup

Figure 3 shows the experimental setup used to demonstrate the proposed scheme using two bulk NLCs. The pump laser system consists of a single-frequency CW Ti:sapphire laser (MBR-110, Coherent) pumped by a diode-pumped solid state (DPSS) laser (Verdi G-10, Coherent) and a resonant frequency doubling unit (MBD-200, Coherent). The output of the Ti:sapphire laser (wavelength: 808 nm; linewidth: approximately 100 kHz) is frequency doubled by second-harmonic generation (SHG) and it is used as the pump beam. The reason why we used a pump laser with narrow linewidth (coherence length longer than 1 km) will be discussed later in Sec. 4.2. The pump beam (wavelength: 404 nm; power: 100 mW) is weakly focused by a lens (focal

#167526 - $15.00 USD Received 26 Apr 2012; revised 18 May 2012; accepted 21 May 2012; published 8 Jun 2012

length: 600 mm); this focusing has a confocal parameter (i.e., twice the Rayleigh length) of approximately 230 mm. Two 2-mm-thick bulk BBO crystals (BBO1 and BBO2) are aligned in parallel along the pump beam with a separation of 10 mm around the focus. The optic axis of BBO1 (BBO2) crystal has a tilt angle of θ_{t1} (θ_{t2}) relative to the cut angle (28.9°) of the BBO crystal. The signal and idler photons generated by type-I phase-matching parametric down conversion are collected by two fiber couplers (FCs) with an emission angle θ of 1° relative to the pump beam. Long pass filters (LPFs) are placed in front of the FCs to filter the pump beam. Collected photons are transferred through polarization-maintaining fibers (PMFs) to the 300-mm spectrograph with a 300-grooves/mm grating blazed at 750 nm (SP-2358, Princeton Instruments) and detected by a charge coupled device (Pixis:100BRX, Princeton Instruments) to measure the frequency spectrum. The phase-matching conditions of the two BBO crystals are controlled by rotating the BBO crystals to vary the tilt angles θ_{t1} and θ_{t2}.

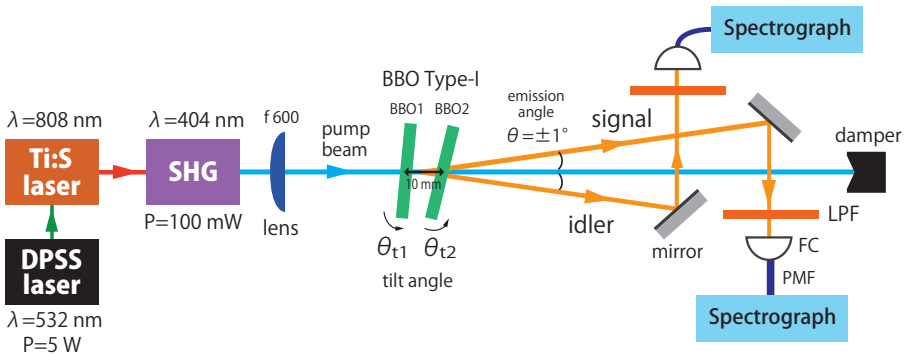

Fig. 3. Experimental setup to measure spontaneous parametric fluorescence spectra generated from one or two BBO crystals (BBO1 and BBO2). θ_{t1} and θ_{t2} are the tilt angles of the optic axes of BBO1 and BBO2 crystals relative to the cut angle, respectively. The two BBO crystals are aligned in parallel along the pump beam with a separation of 10 mm. Generated signal and idler photons are collected at an emission angle of ±1° by fiber couplers and are transferred to the spectrograph to obtain the spectra. DPSS laser: diode-pumped solid-state laser, SHG: second-harmonic generation system, LPF: long pass filter, FC: fiber coupler, PMF: polarization-maintaining fiber.

4. Results and discussion

4.1. Observation of broadband spontaneous parametric fluorescence

To experimentally demonstrate our scheme, we measured spontaneous parametric fluorescence spectra generated from one and two NLCs in the experimental setup shown in Fig. 3. We first measured spontaneous parametric fluorescence spectra generated from only one BBO crystal (BBO2) in a non-collinear configuration for various phase-matching conditions, as shown in Fig. 4(a). The tilt angle θ_{t2} was varied from −0.05° to −0.40° in 0.05° steps. As a result, the spectrum could be controlled by varying the phase-matching conditions, as shown in Fig. 2. The transmission efficiency of the spectrograph was calibrated in these spectra; however, the intensity reduction in the long wavelength region may be due to a reduction in the fiber coupling efficiency. When the tilt angle θ_{t2} was set to −0.05°, the spectrum was degenerate at the center wavelength of 808 nm and the bandwidth (FWHM) was typically 75 nm (34 THz). Thus, a broadband spectrum is expected when spectra with different tilt angles are superimposed. As an example, Fig. 4(b) shows calculated spectra as a superposition of these measured spectra. The bandwidth of the spectra obtained by summing two measured spectra obtained for tilt

#167526 - $15.00 USD Received 26 Apr 2012; revised 18 May 2012; accepted 21 May 2012; published 8 Jun 2012

angles θ_{t2} of -0.05° and -0.15° is approximately 130 nm (60 THz), as plotted by the blue line in Fig. 4(b). A bandwidth of approximately 215 nm (100 THz), which is almost three times that of one degenerate spectrum, can be expected from the sum of four measured spectra with θ_{t2} of -0.10°, -0.20°, -0.30°, and -0.40°, as plotted by the red line in Fig. 4(b).

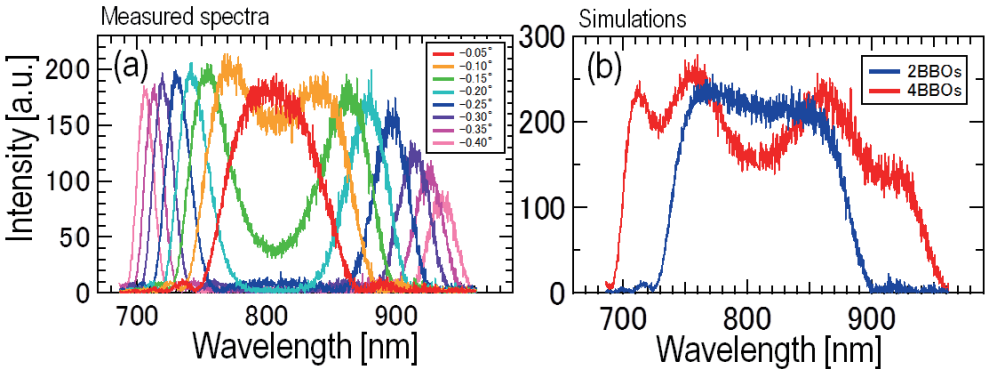

Fig. 4. (a) Measured spontaneous parametric fluorescence spectra generated from one BBO crystal (BBO2) with a tilt angle θ_{t2} varied between -0.05° and -0.40°. (b) Calculated spectra as a superposition of measured spectra of two BBO crystals with θ_{t2} of -0.05° and -0.15° (blue line) and four BBO crystals with θ_{t2} of -0.10, -0.20, -0.30, and -0.40° (red line).

We then measured spectra of both the signal and idler photons of the spontaneous parametric fluorescence generated from both BBO crystals as shown in Fig. 5. A typical bandwidth of 160 nm (73 THz) was obtained with tilt angles θ_{t1} and θ_{t2} of -0.10° and -0.20°, respectively as shown in Fig. 5. A typical single photon count rate was 1.0×10^5 counts per second when the pump beam power was 10 mW. The measured bandwidth was over two times greater than that obtained using only one BBO crystal. This broad bandwidth in the frequency domain corresponds to a Fourier-transform-limited temporal width of approximately 6 fs for correlated photon pairs in the time domain. The intensity ratio of parametric fluorescence collected from two BBO crystals was sensitive to the fiber coupling of the fiber couplers, which was optimized to maximize the overlap of these two spectra. The slight difference between the spectrum of signal (red line in Fig. 5) and idler (blue line in Fig. 5) photons may be caused by the non-perfect spatial mode matching of the two detection modes at the crystal.

Then we measured the coincidence counts between the signal photons and the idler photons for the whole spectrum, i.e. just inserting a low frequency filter (SCF-50S-42L, SIGMA KOKI) to cut the pump beam. With the detection event of the signal photon as a trigger, the coincidence count rate of idler photons was typically 2% that of the single photon count rate. We think this relatively low fraction (2%) is due to technical difficulties when we align single mode fiber couplers. We think the fraction can be improved up to approximately 20% if we can simultaneously monitor the spectra of daughter photons and coincidence counting rate [19].

4.2. Effect of the air gap between the nonlinear crystals in the proposed scheme

In our proposed scheme, there should be gaps between NLCs to control the tilt angles of NLCs, which may affect the phase relation between generated photons and pump photons due to following two causes.

The first cause is the group velocity mismatch between the pump beam and signal (idler) photons. The group velocity mismatch can be evaluated by the dispersion coefficient $D = u_o^{-1} - u_e^{-1}$, where $u_{o,e}$ are the group velocities for ordinary and extraordinary rays in a medium [20].

#167526 - $15.00 USD Received 26 Apr 2012; revised 18 May 2012; accepted 21 May 2012; published 8 Jun 2012

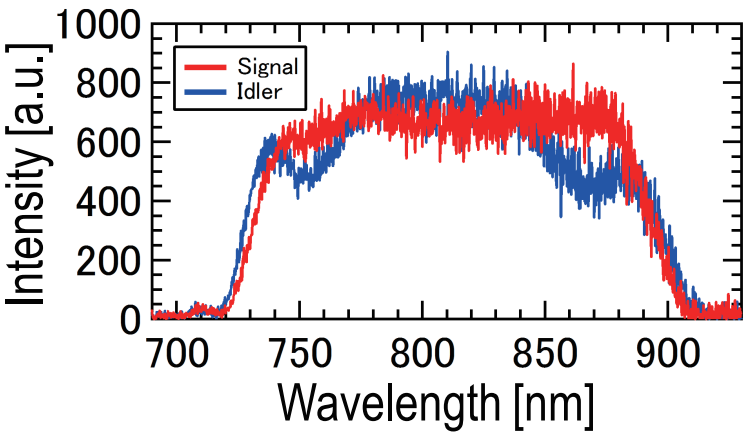

Fig. 5. Measured spectra of signal (red line) and idler (blue line) photons of spontaneous parametric fluorescence generated from two BBO crystals. Spectra of signal and idler photons had measured bandwidths of approximately 160 nm (73 THz). Tilt angles θ_{t1} and θ_{t2} were set to -0.10° and -0.20°, respectively.

Then the spatial separation Δl of the pump and signal (idler) photons after passing through the medium with a length d can be given by $\Delta l = cdD$. If the coherence length of the pump beam is shorter than this separation, this separation causes a loss of the coherence between photons generated from separated multiple NLCs and thus only an incoherent mixture of photons can be obtained [21, 22].

In our experimental setup, two BBO crystals with a length of 2 mm is separated by the air gap with a distance of 10 mm. In this case, the separation Δl in the BBO crystal is approximately 0.1 mm and that in the air gap is less than 1 μm. In our experimental setup shown in Sec. 3, the CW pump laser with a narrow linewidth ($\sim$ 100 kHz) is used. The coherence length of the laser is an order of 1 km and is much longer than these separations (0.1 mm and 1 μm). In this condition, the effect of group velocity mismatch is negligible and it is not necessary to stabilize the distance between crystals with interferometric accuracy. Note that similar condition has been widely used for the polarization-entanglement sources [23–25]. This effect of group velocity mismatch will become critical when one wish to use short pulse lasers with small coherent length for pumping [21, 22].

The second cause is the momentum mismatch between the pump, signal and idler photons. This effect on the polarization entangled photon pair source has been discussed by Atatüre et al. [26] and Giuseppe et al. [20]. For the case of frequency entangled photon pairs generated from the proposed scheme in Sec. 2, the state of photon pairs generated from two NLCs is written by

$$|\Psi>=\int d\Omega F_a(\Omega)|+\Omega>_s|-\Omega>_i+\int d\Omega \exp[i\phi_d(\Omega)]F_b(\Omega)|+\Omega>_s|-\Omega>_i, \qquad (3)$$

where $F_i(+\Omega)=F_i(-\Omega)$ $(i=a,b)$ is a symmetric frequency spectrum of photons generated from ith NLC as explained in Sec. 2 and $\phi_d(\Omega)$ is a phase term. This phase term can be given by $\phi_d(\Omega)=\Delta k(\Omega)d$, where $\Delta k(\Omega)$ is a momentum mismatch between the pump beam, signal and idler photons in the air gap. This momentum mismatch can be written by $\Delta k(\Omega)=k_p-k_s-k_i=n(\omega_p)\omega_p/c-n(\frac{\omega_p}{2}+\Omega)(\frac{\omega_p}{2}+\Omega)/c-n(\frac{\omega_p}{2}-\Omega)(\frac{\omega_p}{2}-\Omega)/c$, where $n(\omega)$ is a refractive index of the air at the frequency ω.

To investigate the effect of this phase term, Here we consider a HOM interferometer [17],

#167526 - $15.00 USD Received 26 Apr 2012; revised 18 May 2012; accepted 21 May 2012; published 8 Jun 2012

with a pair of photons described in Eq. (3). The coincidence rate $P_c(\tau)$ between two separated output ports A and B of the HOM interferometer with the slow single photon detectors can be written by

$$P_c(\tau) \propto \int d\omega_A d\omega_B < \Psi | a_A^\dagger(\omega_A) a_B^\dagger(\omega_B) a_A(\omega_A) a_B(\omega_B) | \Psi > \quad (4)$$

$$= \int d\Omega_A d\Omega_B || < 0 | a_s(\Omega_A) a_i(\Omega_B) e^{i\Omega_B \tau} - a_s(\Omega_B) a_i(\Omega_A) e^{i\Omega_A \tau} | \Psi > ||^2 \quad (5)$$

$$= \int d\Omega | F_a(\Omega) + \exp[i\phi_d(\Omega)] F_b(\Omega) |^2 (1 - \cos(2\Omega\tau)), \quad (6)$$

where τ is a relative time delay between signal and idler photons, $a_j(\omega_j)(j = A, B)$ is an annihilation operator for the mode coupled to the output port $j = A, B$ at the frequency ω_j and $a_j(\Omega_k)(j = s, i$ and $k = A, B)$ is an annihilation operator for the mode of signal ($j = s$) and idler ($j = i$) photons at the frequency Ω_k [27].

Now, let us consider HOM interference signals with the state of photons that have frequency spectra shown in Fig. 6(a), which is a model spectrum based on the experimental data shown in Fig. 4. The spectrum $F_i(\Omega)(i = a, b)$ of photons generated from ith NLC is assumed to be different from each other (cf. Fig. 2). Then a sum of two spectra $F_a(\Omega) + F_b(\Omega)$ has broadened bandwidth ($\Omega/2\pi \sim 70$ THz in this case).

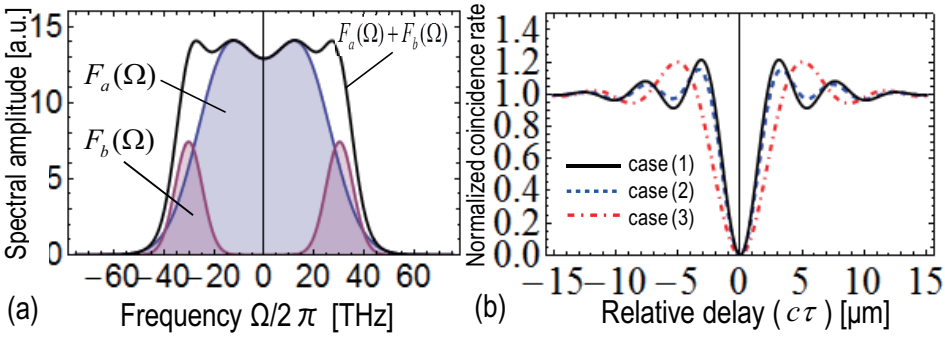

Fig. 6. (a) Frequency spectra $F_i(\Omega)$ of photons generated from ith NLC ($i = a$ (blue line), b (red line)) and a sum of two spectra (black line) with the bandwidth of approximately 70 THz. (b) Coincidence rate $P_c(\tau)$ in a HOM two-photon interferometer with the case (1) $\phi_d = 0$ (solid black line), case (2) $\phi_d \sim 0.37\pi$ (dashed blue line) and case (3) $\phi_d = \pi$ (dashed-dotted red line). The width of the HOM dip with the case (1) is approximately 3 μm

.

Figure 6(b) shows calculated two-photon interference signals of the HOM interferometer for the following three cases: (1) An ideal case with the 0 gap distance (ϕ_d = 0); (2) The case of our experimental condition, with the pump laser wavelength λ_p of 404 nm and the air gap distance d of 10 mm (The average of ϕ_d over the fluorescence spectrum is approximately 0.37 π); (3) The worst case ($\phi_d = \pi$), which corresponds to the air gap distance approximately 27 mm for λ_p of 404 nm. Note that the phase term ϕ_d is a function of the gap distance d between the crystals and refractive indices n of the pump and signal (idler) photons. The results of the calculations for these three cases are shown in Fig. 6(b). The solid black line, the dashed blue line, and the dashed-dotted red line corresponds to case (1), (2), and (3) respectively. In case (1), the HOM interference curve is simply the inverse Fourier transform of the absolute value squared of the sum of the two spectra ($F_a(\Omega) + F_b(\Omega)$), which is shown as the black line in Fig. 6(a). The width of this HOM dip ($c\tau \sim 3$ μm) corresponds to the time correlation of the

#167526 - $15.00 USD Received 26 Apr 2012; revised 18 May 2012; accepted 21 May 2012; published 8 Jun 2012

signal and the idler photon ($\tau \sim 9$ fs). Note that the difference between the dashed blue line (case (2)) and the solid black line (case (1)) is negligibly small. In the worst case (case (3)), the width of the HOM dip is almost the same with the HOM dip given solely by the first crystal ($F_a(\Omega)$). Note that the difference between the curves becomes less significant when the overlap of $F_a(\Omega)$ and $F_b(\Omega)$ become smaller. Note also that this effect caused by momentum mismatch changes has a sinusoidal dependence on the gap distance d, with a period of 54 mm in our experimental condition. Thus, it is not necessary to stabilize the distance between crystals with interferometric accuracy for this effect, too.

In summary in this subsection, we have considered the effect of group velocity mismatch and the momentum mismatch between the pump light and daughter photons on the shape of HOM interference curve. The effect of group velocity mismatch between the pump light and the daughter photon is negligible in the current experimental condition where a CW pump laser with long coherent length is used. The difference in the refractive indices of the air for the pump light and the daughter photons causes the momentum mismatch between the pump light and daughter photons, and it may modify the shape of the HOM interference, but the change is negligibly small for the current experimental condition. The calculated HOM interference curve using a model spectrum considering the experimental data is almost the same with the one calculated for an ideal frequency entangled photon pair. For both of the effects, it is not necessary to stabilize the distance between crystals with interferometric accuracy.

5. Conclusion

We proposed a novel method for generating broadband spontaneous parametric fluorescence by using a set of multiple NLCs. We demonstrated the proposed scheme using two conventional NLCs. The superposition of spontaneous parametric fluorescence spectra generated from two BBO crystals gave a typical bandwidth of 160 nm (73 THz) at the degenerate wavelength of 808 nm. In contrast, the bandwidth with only one BBO crystal was typically 75 nm (34 THz). We also measured coincidence counts of correlated photon pairs generated in a non-collinear configuration. Using this simple scheme, a bandwidth could be broadened by increasing the number of NLCs without employing any special devices, provided the phase-matching conditions of the NLCs are satisfied. Based on a calculation using measured spectra, a bandwidth of approximately 215 nm (100 THz) is expected by using a set of four BBO crystals. Furthermore, the pump laser frequency can be tuned within the tuning range of the NLCs in the proposed method. This tunability is important for applications such as two-photon absorption experiments.

We have also discussed the effect of air gaps between multiple NLCs on the HOM interference between the daughter photons generated by our scheme. Our theoretical analysis suggested that the difference in the refractive indices of the air for the pump light and the daughter photons may modify the shape of the HOM interference, but the change is negligibly small for the current experimental condition. The analysis also suggested that the effect of group velocity mismatch between the pump light and the daughter photon is also negligible and it is not necessary to stabilize the distance between crystals with interferometric accuracy when a pump light with appropriate coherence length is used. The narrow HOM dips of broadband spontaneous parametric fluorescence generated in our scheme are promising for applications such as a quantum optical coherence tomography.

For the generation of broadband parametric fluorescence, higher efficiency may be expected when periodically polled materials are used due to the higher nonlinearities. On the other hand, our scheme has advances on the tunability of both pump and signal/idler wavelengths by simply adjusting the angles of the crystals. It may be also possible to prepare crystals cut at different angles and put together in contact to reduce the dispersion effect when tunability is not nec-

#167526 - $15.00 USD Received 26 Apr 2012; revised 18 May 2012; accepted 21 May 2012; published 8 Jun 2012

essary. The limit of the bandwidth is, in principle, given by the phase matching condition and transparent window of the nonlinear crystal. However, the increase in number of crystals to achieve very broad spectrum may suffer from technical difficulties like fine adjustment of each crystals.

Our scheme could also be useful for conventional nonlinear optics especially with the process of the second harmonic generation, which is an inverse process of the parametric down-conversion. The second harmonic generation from broadband anti-correlated frequencies have recently been demonstrated by classical laser pulses for optical coherence tomography [28,29].

Acknowledgments

This work was supported in part by Grant-in-Aids from the JST-CREST Project, JSPS, the Quantum Cybernetics Project, the FIRST Program of JSPS, the Project for Developing Innovation Systems of MEXT, the GCOE program, and the Research Foundation for Opto-Science and Technology.

#167526 - $15.00 USD Received 26 Apr 2012; revised 18 May 2012; accepted 21 May 2012; published 8 Jun 2012